

# Molecular Basis for the Catalytic Specificity of the CTX-M Extended-Spectrum $\beta$ -Lactamases

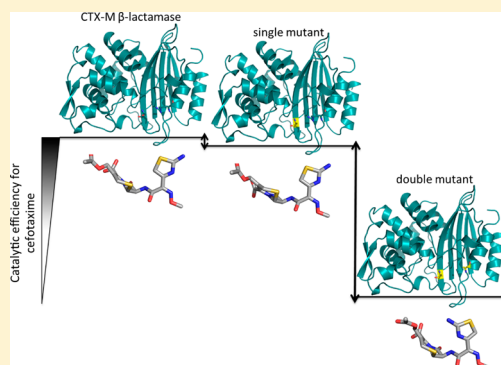
Carolyn J. Adamski,<sup>†,‡</sup> Ana Maria Cardenas,<sup>†,‡</sup> Nicholas G. Brown,<sup>†</sup> Lori B. Horton,<sup>‡</sup> Banumathi Sankaran,<sup>§</sup> B. V. Venkataram Prasad,<sup>†,‡</sup> Hiram F. Gilbert,<sup>†</sup> and Timothy Palzkill<sup>\*,†,‡,§,||</sup>

<sup>†</sup>Verna and Marrs McLean Department of Biochemistry and Molecular Biology, <sup>‡</sup>Department of Molecular Virology and Microbiology, <sup>||</sup>Department of Pharmacology, Baylor College of Medicine, One Baylor Plaza, Houston, Texas 77030, United States

<sup>§</sup>Berkeley Center for Structural Biology, Lawrence Berkeley National Laboratory, Berkeley, California 94720, United States

## S Supporting Information

**ABSTRACT:** Extended-spectrum  $\beta$ -lactamases (ESBLs) pose a threat to public health because of their ability to confer resistance to extended-spectrum cephalosporins such as cefotaxime. The CTX-M  $\beta$ -lactamases are the most widespread ESBL enzymes among antibiotic resistant bacteria. Many of the active site residues are conserved between the CTX-M family and non-ESBL  $\beta$ -lactamases such as TEM-1, but the residues Ser237 and Arg276 are specific to the CTX-M family, suggesting that they may help to define the increased specificity for cefotaxime hydrolysis. To test this hypothesis, site-directed mutagenesis of these positions was performed in the CTX-M-14  $\beta$ -lactamase. Substitutions of Ser237 and Arg276 with their TEM-1 counterparts, Ala237 and Asn276, had a modest effect on cefotaxime hydrolysis, as did removal of the Arg276 side chain in an R276A mutant. The S237A:R276N and S237A:R276A double mutants, however, exhibited 29- and 14-fold losses in catalytic efficiency for cefotaxime hydrolysis, respectively, while the catalytic efficiency for benzylpenicillin hydrolysis was unchanged. Therefore, together, the Ser237 and Arg276 residues are important contributors to the cefotaximase substrate profile of the enzyme. High-resolution crystal structures of the CTX-M-14 S70G, S70G:S237A, and S70G:S237A:R276A variants alone and in complex with cefotaxime show that residues Ser237 and Arg276 in the wild-type enzyme promote the expansion of the active site to accommodate cefotaxime and favor a conformation of cefotaxime that allows optimal contacts between the enzyme and substrate. The conservation of these residues, linked to their effects on structure and catalysis, imply that their coevolution is an important specificity determinant in the CTX-M family.



A wide range of bacterial infectious diseases are treated with  $\beta$ -lactam antibiotics. Unfortunately, resistant bacteria have evolved mechanisms to escape the lethal action of these drugs. The majority of resistance to  $\beta$ -lactam antibiotics results from the expression of  $\beta$ -lactamases, which are enzymes that hydrolyze the amide bond of the  $\beta$ -lactam ring of the drugs to inactivate these antimicrobials.<sup>1</sup>

In the early 1980s, extended-spectrum oxyimino-cephalosporins, including cefotaxime, were developed that are poor substrates for class A serine  $\beta$ -lactamases such as TEM-1 and SHV-1.<sup>2–4</sup> These antibiotics are characterized by bulky side chains containing an oxyimino group and, for many, an aminothiazole ring (Figure 1).<sup>5</sup> The extensive clinical use of these antibiotics has resulted in the emergence of extended-spectrum  $\beta$ -lactamases (ESBLs), which are class A enzymes capable of hydrolyzing these drugs.

The CTX-M family of class A ESBLs first appeared in the late 1980s and has since become the most widespread plasmid-mediated source of resistance to oxyimino-cephalosporins in Gram-negative bacteria.<sup>4,6</sup> The CTX-M-14  $\beta$ -lactamase is a common CTX-M-type enzyme among antibiotic resistant bacteria.<sup>3</sup> It was initially found in isolates of *Klebsiella*

*pneumoniae*, *Shigella sonnei*, and *Escherichia coli* and has been isolated from a large range of clinical bacteria, mainly from the Enterobacteriaceae family.<sup>3</sup> A defining feature of the CTX-M enzymes is that they hydrolyze the oxyimino-cephalosporin, cefotaxime, with approximately 1000-fold higher catalytic efficiency ( $k_{\text{cat}}/K_{\text{m}}$ ) than other class A  $\beta$ -lactamases such as TEM-1 and SHV-1.<sup>4</sup> Although the overall folds are structurally similar, the CTX-M enzymes share less than 40% amino acid sequence identity with TEM-1 and SHV-1.<sup>4</sup> The nature of the catalytic and structural features of the CTX-M enzymes responsible for their high activity toward cefotaxime is an important question. Structural analysis of variants of the TEM and SHV enzymes capable of hydrolyzing oxyimino-cephalosporins showed that the substitutions act on the omega loop or the  $\beta$ 3 strand that outline the active site to increase the active site volume to accommodate the larger cefotaxime and ceftazidime substrates.<sup>7,8</sup> X-ray structures of CTX-M enzymes with and without substrate revealed a narrow active site that

Received: September 23, 2014

Revised: November 23, 2014

Published: December 9, 2014

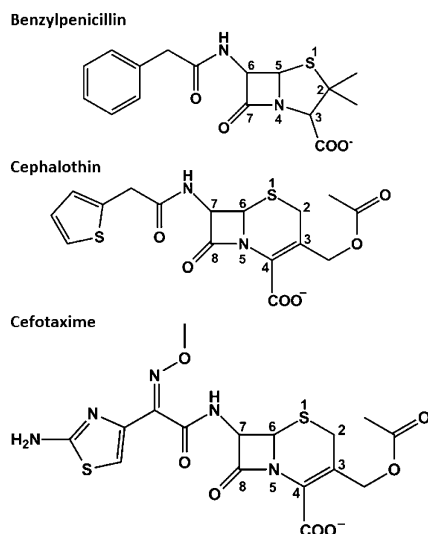


**Figure 1.** Structures of  $\beta$ -lactam antibiotics. Cefotaxime, cephalothin, and benzylpenicillin with atom positions numbered.

expands significantly due to a conformational change upon cefotaxime binding.<sup>5,9,10,11</sup> This expansion is accompanied by the rupture of a hydrogen bond between main chain groups of Asn170 and Asp240 that connects the omega loop to the  $\beta$ 3 strand.<sup>11</sup>

Despite the lack of overall high sequence identity, the majority of the active site residues that make contact with substrate in TEM-1 and CTX-M-14 are identical or represent conservative changes.<sup>12–14</sup> Of the remaining positions, two stand out as differences that may contribute to the enhancement of the cefotaximase activity in the CTX-M family. In the TEM/SHV-type enzymes, a conserved arginine residue at position 244 interacts with the C-3/4 carboxyl group common to  $\beta$ -lactam antibiotics to stabilize the substrate and transition state complexes of benzylpenicillin<sup>15,16,17</sup> (Figure 2). In the CTX-M family, this arginine is replaced by Thr244, but a different positive charge is present in the region due to an arginine at position 276. In the TEM-1/SHV-1 enzymes, position 276 is occupied by an asparagine<sup>5,9</sup> (Table 1 and Figure 2). However, substitution of the analogous Arg276 with a number of amino acids in the CTX-M-4 or CTX-M-1 enzymes has little effect on penicillin G and cephalothin hydrolysis and only a modest (2–3-fold) effect on the hydrolysis of cefotaxime.<sup>13,18</sup> These results suggest a relatively minor contribution of Arg276 toward determining the substrate specificity, despite the fact that it is conserved throughout the CTX-M family.

The CTX-M enzymes contain a serine at position 237, whereas this position is an alanine in TEM/SHV enzymes (Table 1 and Figure 2). X-ray structures of a CTX-M-9 S70G mutant in complex with benzylpenicillin or cefotaxime show that Ser237 makes contact with cefotaxime, including a hydrogen bond with the C-4 carboxyl group. However, Ser237 does not contact bound benzylpenicillin.<sup>11</sup> A S237A substitution in CTX-M-4 resulted in little effect on benzylpenicillin hydrolysis but, surprisingly, also showed only a modest decrease in activity for cefotaxime hydrolysis.<sup>19</sup>

The sequence conservation among the CTX-M family and the prior structural observations suggest that Arg276 and Ser237 would contribute significantly to the enhanced specificity of this family toward cefotaxime. Thus, the rather

modest effect of the individual mutations on cefotaxime hydrolysis is unexpected. Because of their conservation in the CTX-M family and the structural differences in this region compared to the TEM-type enzymes, we hypothesized that the two residues might interact cooperatively so that mutating both residues in the same molecule would have a larger effect on catalysis than expected from the individual mutations.<sup>14</sup> In this study, we tested this hypothesis by constructing single and double mutant combinations of residues 237 and 276 in CTX-M-14  $\beta$ -lactamase and assessed kinetic and structural effects of the mutations with first-generation and extended-spectrum antibiotics. The kinetic and structural results argue that these two conserved residues in the CTX-M family work together to position the substrate and significantly enhance cefotaxime hydrolysis.

## MATERIALS AND METHODS

**Bacterial Strains and Plasmids.** *E. coli* K12 XL1-Blue strain (*recA1 endA1 gyrA96 thi-1 hsdR17 supE44 relA1 lac* [F' *proAB lacI<sup>q</sup>Z $\Delta$ M15 Tn10* (Tet<sup>r</sup>)] was obtained from Stratagene (La Jolla, CA) and used in site-directed mutagenesis experiments. The *E. coli* RB791 strain was used for protein expression and purification. The *bla*<sub>CTX-M-14</sub> gene was inserted into the pTP123 plasmid, and the resulting plasmid was used as template for site-directed mutagenesis and subsequent expression of mutant enzymes in *E. coli* RB791.<sup>14</sup>

**Site-Directed Mutagenesis.** All CTX-M-14 mutants were created using the QuikChange kit (Stratagene, La Jolla, CA). Primers were obtained from Integrated DNA Technologies (Coralville, IA). The following primers introduced the underlined mutations into pTP123 CTX-M-14 (complementary primer not shown):

- S237A (5'-gtgataagaccg<sup>g</sup>cgccg<sup>g</sup>cgactacggca-3');  
 R276A (5'-cgcagagagccg<sup>g</sup>cccgatgtctgct-3');  
 R276N (5'-cgcagagagccg<sup>g</sup>caatgatgtctgct-3').

All CTX-M-14 mutant constructs were verified by DNA sequencing (Lone Star Laboratories, Houston, TX).

**Determination of Minimum Inhibitory Concentrations.** *In vivo* antibiotic resistance levels were determined by E-test (Ab Biodisk, Sweden) in accordance with the manufacturer's recommendations to evaluate the function of CTX-M-14 mutants in *E. coli* RB791 cells. Cultures were inoculated with a single colony and grown overnight at 37 °C. Overnight cultures were diluted 1:100 and plated on LB agar. An E-test strip was then added to a single plate, which was placed at 37 °C overnight before the resistance level was recorded.

**Protein Purification.** *E. coli* RB791 cells transformed with the relevant pTP123 CTX-M-14 construct were selected on LB agar containing 12.5  $\mu$ g/mL chloramphenicol. Single colonies were used to inoculate 20 mL of LB supplemented with 12.5  $\mu$ g/mL chloramphenicol, and cultures were grown overnight at 37 °C. Fifteen milliliters of the overnight culture was used to inoculate 1.5 L of LB containing 12.5  $\mu$ g/mL chloramphenicol, and the resulting cultures were allowed to grow to mid log (OD<sub>600</sub> ~ 0.7). The cultures were grown at 23 °C overnight after addition of 300  $\mu$ L of 1 M IPTG to the 1.5 L cultures, resulting in a final concentration of 0.2 mM. Cells were harvested by centrifugation and frozen for at least an hour at -80 °C. To release the periplasmic contents, the cells were resuspended in 30 mL of 10 mM Tris, pH 8.0, 20% sucrose, and 1 mM EDTA and incubated on ice. After 20 min, 40 mL of cold, sterile water was added and mixed. The insoluble material

was pelleted by centrifugation. The supernatant was filtered and passed through a HiTrap SP column (Amersham, GE Healthcare, Piscataway, NJ). A linear NaCl gradient was used to elute the CTX-M-14 enzyme. The purity of the  $\beta$ -lactamase containing fractions was determined by SDS-PAGE, and the pooled fractions were dialyzed overnight into 50 mM sodium phosphate buffer, pH 7.0. The concentration of active  $\beta$ -lactamase was determined by titrating the CTX-M-14 enzyme with  $\beta$ -lactamase inhibitory protein-II (BLIP-II), which is a potent inhibitor ( $0.5 \text{ pM } K_i$ ) of the CTX-M-14 enzyme.<sup>20</sup> Varying concentrations ( $\mu\text{M}$ ) of BLIP-II were incubated with CTX-M-14 enzyme for 30 min at room temperature in a 96-well plate in a total volume of  $200 \mu\text{L}$ . Following incubation, the chromogenic substrate nitrocefin was added to a final concentration of  $30 \mu\text{M}$ , and the initial velocity of nitrocefin hydrolysis was followed by absorbance at 482 nm using a plate reader to determine the percent BLIP-II occupancy of  $\beta$ -lactamase (Tecan Infinite 200 PRO, Männedorf, Switzerland). The percent inhibition versus inhibitor concentration was fit with a linear equation and extrapolated to 100% inhibition to obtain the active enzyme concentration.<sup>21</sup>

**Enzyme Kinetics.** Steady-state Michaelis–Menten kinetic parameters were determined on a Beckman-Coulter spectrophotometer model DU 800 (Fullerton, CA). Substrate hydrolysis was monitored at the following wavelengths: benzylpenicillin, 233 nm; cefotaxime, 264 nm; cephalothin, 262 nm; nitrocefin, 482 nm. Reactions were performed in 50 mM sodium phosphate buffer, pH 7.0, with 1 mg/mL BSA at  $30^\circ\text{C}$ . BSA was added to buffer in order to stabilize  $\beta$ -lactamase, which is present at low concentrations in enzyme assays. BSA was excluded for the benzylpenicillin reactions due to an overlap in protein absorbance with the wavelength used to monitor the reaction. To determine  $K_m$  and  $k_{\text{cat}}$  values, initial velocity rates were fitted over a range of substrate concentrations to a Michaelis–Menten curve using GraphPad Prism 6, and standard errors to these fits are reported. The errors reported for  $k_{\text{cat}}/K_m$  are calculated by summing the percent errors of both parameters.

**Determination of Statistical Significance for  $k_{\text{cat}}/K_m$  values.** Enzymatic efficiency ( $k_{\text{cat}}/K_m$ ) was determined as previously described, and significance was determined using GraphPad Prism 6 unpaired *t*-test for the CTX-M-14 as compared to the various mutants. \*\* denotes a *p*-value less than 0.005, and \*\*\* denotes a *p*-value less than 0.0005.

**$\Delta\Delta G$  Calculations.**  $\Delta\Delta G$  was calculated using the following equation

$$\Delta\Delta G = -RT \ln \frac{(k_{\text{cat}}/K_m)_{\text{wild type}}}{(k_{\text{cat}}/K_m)_{\text{mutant}}} \quad (1)$$

Using this equation, an increase in catalytic efficiency ( $k_{\text{cat}}/K_m$ ) upon mutation would result in a negative  $\Delta\Delta G$  value, whereas a decrease in catalytic efficiency would be reported as a positive change in free energy. Error for  $\Delta\Delta G$  values was calculated using the following equation

$$\Delta\Delta G \text{ error} = \Delta\Delta G \sqrt{\frac{\text{SEM}}{k_{\text{cat}}/K_m(\text{WT})} + \frac{\text{SEM}}{k_{\text{cat}}/K_m(\text{mut})}} \quad (2)$$

where SEM represents standard error of the mean, WT represents wild-type CTX-M-14, and mut represents the mutant enzyme.

**Fluorescence Scan of CTX-M-14 and Mutants.** A fluorescence scan was performed on CTX-M-14 as well as

CTX-M-14 S237A and CTX-M-14 S237A:R276A to ensure no secondary structural changes occurred in the mutant structures. This was also done to ensure that the crystal structures accurately depicted the structures seen in bulk solution. The protein was diluted to  $2 \mu\text{M}$  in 50 mM sodium phosphate buffer, pH 7.0. The protein was excited at 280, and fluorescence intensity was measured from 295 to 545 nm using a Cary Eclipse Fluorescent Spectrophotometer from Agilent Technologies (Santa Clara, CA). The fluorescence intensity was normalized for all measurements, and each protein was measured in at least duplicate.

**Crystallization and Structure Determination.** The CTX-M-14 S70G, S70G:S237A, and S70G:S237A:R276A proteins were dialyzed into 5 mM Tris, pH 7.0, and 50 mM NaCl and were concentrated to 10 mg/mL for crystallization. Diffraction-quality crystals were obtained in 30% PEG4K containing 0.2 M ammonium sulfate. The protein and mother liquor were mixed at a 1:1 ratio in a  $2 \mu\text{L}$  drop and grown by hanging drop vapor diffusion. The crystals were harvested and cryoprotected with 25% glycerol added to the mother liquor. For the structures in complex with cefotaxime, crystals were soaked in the mother liquor at pH 8.0 (adjusted with 1 M Tris) containing 50 mM cefotaxime overnight and then cryoprotected in 25% glycerol, 50 mM cefotaxime, 30% PEG4K, 0.2 M ammonium sulfate, pH 8.0. X-ray diffraction data sets were collected on beamline 5.0.2 (Advanced Light Source, Berkeley, CA) for all structures except CTX-M-14 S70G, which was collected at Baylor College of Medicine. The data sets for S70G and S70G:S237A were processed using iMosfilm, and the MolRep program from CCP4 was used for molecular replacement using CTX-M-14 (1YLT) as the search model.<sup>22–24</sup> The diffraction data sets for S70G:S237A:R276A were processed with HKL2000 software, and the Phaser program from the CCP4 package was used for molecular replacement using the wild-type CTX-M-14 (1YLT) as the search molecule.<sup>25,26</sup> One molecule was found in the asymmetric unit for all crystals. All models were fitted to the density in Coot.<sup>27</sup> The structures were continually refined through the use of Coot and Phenix using default anisotropic corrections. Ordered solvent was added in Coot. Structures were analyzed using the LigPlot+ program.<sup>28</sup> Hydrogen bond and hydrophobic interactions were analyzed using Ligplus with distance criterion of 2.6 and 3.3 Å for hydrogen bonds and carbon–carbon distance of 3.6 and 4.5 Å for hydrophobic interactions. Molecular graphics images for Figures 3 and 4 were generated using PyMOL v1.3.<sup>29</sup> Molecular graphics images for Figure 5 were produced using the UCSF Chimera package from the Computer Graphics Laboratory, University of California, San Francisco (supported by NIH P41 RR-01081).<sup>30</sup>

## RESULTS

**Contributions of Ser237 and Arg276 to  $\beta$ -Lactamase Hydrolysis.** Although most of the active site residues are conserved between the TEM-1/SHV-1 penicillinases and CTX-M  $\beta$ -lactamases, residues Ser237 and Arg276 differ from their counterparts in TEM-1/SHV-1 (Table 1 and Figure 2). On the basis of this, it was hypothesized that Ser237 and Arg276 contribute to the specificity of CTX-M enzymes for cefotaxime hydrolysis. To test this idea, the mutations S237A, R276N, and R276A were introduced singly and in combination into the CTX-M-14 enzyme. The S237A and R276N substitutions convert these positions to the equivalent TEM-1 residue,

**Table 1. Amino Acid Residues at Positions 237, 244, and 276 in the Representative Penicillinase and CTX-M Family  $\beta$ -Lactamases**

	237	244	276
TEM-1 (1M40 <sup>a</sup> )	Ala	Arg	Asn
SHV-2 (1N9B)	Ala	Arg	Asn
CTX-M-1 <sup>b</sup>	Ser	Thr	Arg
CTX-M-2	Ser	Thr	Arg
CTX-M-8	Ser	Thr	Arg
CTX-M-25	Ser	Thr	Arg
CTX-M-9 (1YLW)	Ser	Thr	Arg
CTX-M-14 (1YLT)	Ser	Thr	Arg

<sup>a</sup>PDB codes are provided in parentheses for available structures.

<sup>b</sup>CTX-M-1, 2, 8, 9, and 25 are representative enzymes from each subgroup of CTX-M- $\beta$ -lactamases. CTX-M-14 is a member of the CTX-M-9 subgroup.

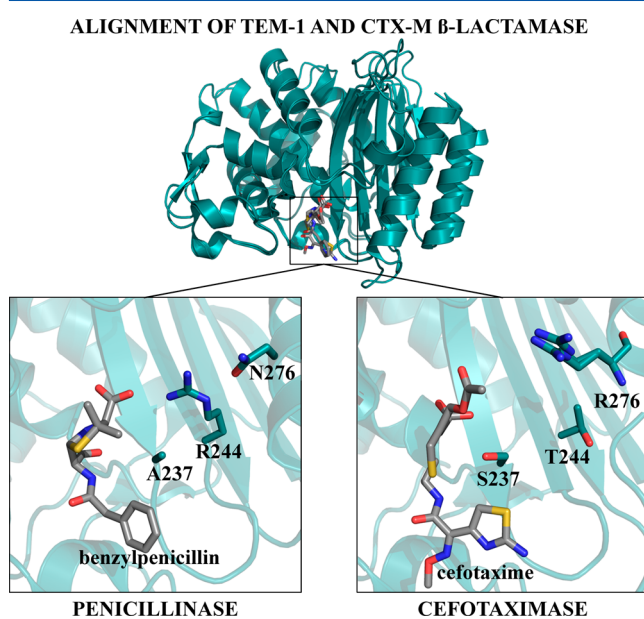


**Figure 2.** View of residue positions 237, 244, and 276 in the TEM-1 and CTX-M  $\beta$ -lactamases. A structural alignment between TEM-1  $\beta$ -lactamase (PDB ID: 1FQG) and CTX-M-9  $\beta$ -lactamase (PDB ID: 3HLW) is shown in teal cartoon with ligands shown as gray sticks. The left panel shows residues Ala237 and Arg244 and Asn276 in TEM-1  $\beta$ -lactamase (teal ribbon) with benzylpenicillin (gray sticks) in the active site. The TEM-1  $\beta$ -lactamase is representative of class A enzymes that efficiently hydrolyze penicillins and early generation cephalosporins. In TEM-1  $\beta$ -lactamase, Arg244 is directed toward the carboxyl group of benzylpenicillin. The right panel shows residues Ser237, Thr244, and Arg276 in CTX-M-9  $\beta$ -lactamase (teal ribbon) with cefotaxime (gray sticks) in the active site. The hydroxyl group of Ser237 forms a hydrogen bond with the C4 carboxylate of cefotaxime. Arg276 is directed toward the C3 methyl acetate group and the C4 carboxylate of cefotaxime, although it does not make direct interactions with these groups. Enzymes are shown in teal, with their respective ligands shown as gray sticks. Nitrogen atoms are shown in blue, oxygen atoms are shown in red, and sulfur atoms are shown in yellow.

whereas R276A was introduced to test the impact of removing both positive charge and all hydrogen-bonding capacity from the side chain.

To test the *in vivo* activity of the CTX-M-14 mutant enzymes, minimum inhibitory concentrations (MICs) were evaluated in *E. coli* with plasmids encoding the various mutants (Supporting Information Table S1). MICs were determined for

benzylpenicillin, cephalothin, and cefotaxime substrates. The S237A mutant caused a decrease in resistance levels for cefotaxime, but it showed no change in resistance levels for benzylpenicillin or cephalothin. Similar results were seen for the R276A and R276N single mutants and the S237A:R276A double mutant. The S237A:R276N double mutant caused no change in resistance levels for benzylpenicillin, but it showed decreased resistance levels for both cephalothin and cefotaxime. Overall, these results suggest that positions 237 and 276 play an important role in the activity of CTX-M-14 enzyme for cefotaxime and less pronounced roles in the activity toward benzylpenicillin and cephalothin (Supporting Information Table S1).

After expression in *E. coli* and purification, the steady-state kinetic parameters  $k_{\text{cat}}$ ,  $K_m$ , and  $k_{\text{cat}}/K_m$  were determined for the three substrates benzylpenicillin, cephalothin, and cefotaxime (Table 2). The kinetic parameter  $k_{\text{cat}}/K_m$  reflects the hydrolysis of substrate under conditions where the substrate concentration is low compared to the  $K_m$ , a situation that is likely to reflect the specificity of the enzyme *in vivo*. In contrast,  $k_{\text{cat}}$  reflects the conversion of bound substrate to product under saturating conditions, an indicator of how a mutation affects the energetics of the enzyme–substrate complex compared to the enzyme–transition state complex.

The S237A substitution in CTX-M-14 shifted the substrate specificity to improve catalytic efficiency for benzylpenicillin hydrolysis and decrease cefotaxime hydrolysis (*p*-value of 0.001 when compared to wild-type), consistent with an alanine at position 237 in the TEM-1/SHV-type enzymes that hydrolyze cefotaxime slowly (Table 2 and Supporting Information Figure S1). The substitution of R276A or R276N had little impact on the kinetic parameters for benzylpenicillin hydrolysis and also decreased catalytic efficiency for cefotaxime hydrolysis by 3–6-fold (*p*-values less than 0.001 when compared to wild-type) (Table 2 and Supporting Information Figure S1). The R276A and R276N results suggest the loss of positive charge, rather than a loss of a hydrogen bond or other side chain contacts, accounts for the decreased hydrolysis of cefotaxime for the Arg276 mutants (Table 2).

**Effects of Double Mutants.** Since Ser237 and Arg276 are both conserved in the CTX-M family, mutations of both side chains (S237A:R276A or S237A:R276N) were introduced at the same time. The effects of the double mutations on the kinetic parameters for benzylpenicillin, cephalothin, and cefotaxime hydrolysis are shown in Table 2. For benzylpenicillin hydrolysis, neither of the double mutants had an effect on  $k_{\text{cat}}/K_m$ , but both increased  $k_{\text{cat}}$  by about 4-fold. The increases in  $k_{\text{cat}}$  suggest that the Ser237 and Arg276 side chains together inhibit turnover of benzylpenicillin once substrate is bound to CTX-M-14.

In contrast, the S237A:R276A double mutant exhibits a 4-fold reduction in  $k_{\text{cat}}/K_m$  for cephalothin hydrolysis and a 14-fold decrease in  $k_{\text{cat}}/K_m$  for cefotaxime (*p*-value of 0.0002 when compared to wild-type) (Table 2 and Supporting Information Figure S1). The S237A:R276N mutations caused a 4-fold decrease in  $k_{\text{cat}}/K_m$  for cephalothin and a larger, 29-fold, decrease in  $k_{\text{cat}}/K_m$  for cefotaxime (*p*-value of 0.0002 when compared to wild-type) (Supporting Information Figure S1). Therefore, the 237 and 276 side chains together enhance the hydrolysis of cephalosporin antibiotics but have only small effects on the hydrolysis of benzylpenicillin. Furthermore, the effects of the mutations on  $k_{\text{cat}}/K_m$  are significantly larger for the oxymino-cephalosporin cefotaxime versus cephalothin

Table 2. Kinetic Parameters of CTX-M-14  $\beta$ -Lactamase and Mutant Enzymes

	CTX-M-14	S237A	R276A	R276N	S237A:R276A	S237A:R276N
Benzylpenicillin						
$K_m$ ( $\mu\text{M}$ ) <sup>a</sup>	36 ± 4	38 ± 6	46 ± 11	45 ± 5	136 ± 6	118 ± 8
$k_{\text{cat}}$ ( $\text{s}^{-1}$ ) <sup>a</sup>	179 ± 6	373 ± 16	176 ± 13	204 ± 6	838 ± 13	850 ± 21
$k_{\text{cat}}/K_m$ ( $\mu\text{M}^{-1} \text{s}^{-1}$ ) <sup>b</sup>	5.0 ± 0.7	9.8 ± 2	3.8 ± 1	4.5 ± 0.6	6.2 ± 0.4	7.2 ± 0.7
Cephalothin						
$K_m$ ( $\mu\text{M}$ ) <sup>a</sup>	88 ± 21	75 ± 12	264 ± 30	196 ± 17	140 ± 12	175 ± 11
$k_{\text{cat}}$ ( $\text{s}^{-1}$ ) <sup>a</sup>	1429 ± 96	997 ± 43	2493 ± 110	1580 ± 52	532 ± 16	522 ± 12
$k_{\text{cat}}/K_m$ ( $\mu\text{M}^{-1} \text{s}^{-1}$ ) <sup>b</sup>	16 ± 5	13 ± 3	9 ± 1	8 ± 1	3.8 ± 0.4	3.0 ± 0.3
Cefotaxime						
$K_m$ ( $\mu\text{M}$ ) <sup>a</sup>	60 ± 9	151 ± 11	88 ± 10	119 ± 8	737 ± 87	770 ± 68
$k_{\text{cat}}$ ( $\text{s}^{-1}$ ) <sup>a</sup>	175 ± 8	173 ± 5	86 ± 2	56 ± 2	122 ± 9	94 ± 5
$k_{\text{cat}}/K_m$ ( $\mu\text{M}^{-1} \text{s}^{-1}$ ) <sup>b</sup>	2.9 ± 0.2	1.1 ± 0.1	1.0 ± 0.1	0.50 ± 0.05	0.20 ± 0.04	0.10 ± 0.01

<sup>a</sup>Errors reported for this parameter are the standard error of the mean calculated from multiple experiments. <sup>b</sup>Errors reported for this parameter are calculated by summing the percent errors of  $K_m$  and  $k_{\text{cat}}$ .

Table 3. Free Energy Values and Additivity Relationships between Single and Double Mutants for  $k_{\text{cat}}/K_m$ 

		S237A	R276A	S237A:R276A	$\Delta G_I$
$\Delta\Delta G_{k_{\text{cat}}/K_m}$ (kcal/mol)	benzylpenicillin	-0.40 ± 0.9	0.17 ± 0.05	-0.13 ± 0.02	0.1
	cephalothin	0.12 ± 0.04	0.3 ± 0.1	0.9 ± 0.3	0.4
	cefotaxime	0.58 ± 0.06	0.64 ± 0.07	1.6 ± 0.3	0.4
		S237A	R276N	S237A:R276N	$\Delta G_I$
$\Delta\Delta G_{k_{\text{cat}}/K_m}$ (kcal/mol)	benzylpenicillin	-0.4 ± 0.9	0.06 ± 0.01	-0.22 ± 0.04	0.1
	cephalothin	0.12 ± 0.04	0.4 ± 0.1	1.0 ± 0.3	0.5
	cefotaxime	0.58 ± 0.06	1.0 ± 0.1	2.0 ± 0.1	0.4

hydrolysis (Supporting Information Figure S1). In the double mutant, replacing Arg276 with either asparagine or alanine has a similar effect on catalysis for all substrates, implying a role for positive charge at position 276 on the observed effects.

An interesting finding to emerge from the kinetic analysis of the S237A:R276A/N double mutants is that introducing both mutations into the CTX-M-14 enzyme at the same time decreases its selectivity toward cefotaxime compared to that for cephalothin and benzylpenicillin. Since Ser237 and Arg276 are conserved among the CTX-M enzymes, the results indicate these positions are important determinants of the ESBL-properties of CTX-M  $\beta$ -lactamases.

The fact that Ser237 and Arg276 appear together among CTX-M enzymes suggests they may work together to facilitate catalysis and, therefore, that the mutations at these positions may be coupled and nonadditive. The change in a functional property ( $k_{\text{cat}}/K_m$ , in this case) caused by a single mutation at sites X and Y can be expressed relative to the wild-type enzyme as  $\Delta\Delta G_{(X)}$  and  $\Delta\Delta G_{(Y)}$ .<sup>31</sup> Similarly, the  $\Delta\Delta G_{(X,Y)}$  represents the free energy differences between wild-type and the double mutant. In the absence of any cooperativity, the free energy difference of the double mutant is expected to be the sum of the free energy changes of the single mutants. However, if there is an interaction between the two, then the observed effect of the double mutant is given by

$$\Delta\Delta G_{(X,Y)} = \Delta\Delta G_{(X)} + \Delta\Delta G_{(Y)} + \Delta G_I \quad (3)$$

where  $\Delta G_I$  represents the coupling free energy. The sign of the coupling free energy indicates whether the cooperativity serves to increase or decrease the observed activity relative to the wild-type.<sup>31</sup>

Analysis of the double mutant cycles for the catalytic efficiency toward the antibiotics tested reveals larger  $\Delta G_I$  values for the cephalosporins, cephalothin and cefotaxime, than for

benzylpenicillin (Table 3). Mutations at positions 237 and 276, whether singly or in combination, have small effects (<2-fold) on the  $k_{\text{cat}}/K_m$  values for the hydrolysis of benzylpenicillin. For the cephalosporins cephalothin and cefotaxime, however, the combined mutations act cooperatively to reduce catalytic efficiency of the double mutants more than expected based on adding the effects of the single mutants (Table 3). For cefotaxime hydrolysis, the single mutation S237A decreases  $k_{\text{cat}}/K_m$  by 3-fold, and the R276N mutation decreases it by 6-fold. If the two mutations were additive, then the double mutant would be expected to decrease the  $k_{\text{cat}}/K_m$  for cefotaxime by 18-fold; however, the observed decrease was 29-fold, larger than expected based on simple additivity. Similarly, based on the single mutants, the S237A:R276A double mutant would be expected to decrease the  $k_{\text{cat}}/K_m$  for cefotaxime by 7.6-fold; however, the observed decrease was 14-fold. Thus, residues Ser237 and Arg276 work together cooperatively to facilitate cefotaxime hydrolysis.

**X-ray Structure Determination of the CTX-M-14 Mutant Enzymes.** To investigate the structural basis behind the changes in the substrate specificity for cefotaxime hydrolysis by the single and double mutant enzymes, the crystal structures of the CTX-M-14 S70G single mutant, S70G:S237A double mutant, and S70G:S237A:R276A triple mutant were determined alone and in complex with cefotaxime (Table 4 and Figure 3). The substitution of the Ser70 nucleophilic residue with glycine was included in order to visualize bound substrate in the active site in the absence of catalysis.<sup>11</sup> The S70G substitution did not significantly alter the shape of the catalytic pocket in the apo form, as evidenced by a root-mean-square deviation (RMSD) of 0.21, 0.18, and 0.18 Å for the matching  $\text{C}\alpha$  atoms of the residues in the active site that form hydrogen bonds with substrate between the wild-type CTX-M-14 enzyme (PDB ID: 1YLT) with the S70G, S70G:S237A, and

Table 4. Crystallographic Data Refinement and Statistics

	CTX-M-14 S70G	CTX-M-14 S70G:S237A	CTX-M-14 S70G:S237A: R276A	CTX-M-14 S70G-cefotaxime	CTX-M-14 S60G:S237A-cefotaxime	CTX-M-14 S70G:S237A: R276A-cefotaxime
Data Collection						
space group	P2 <sub>1</sub> -2 <sub>1</sub> -2 <sub>1</sub>					
<i>a</i> , <i>b</i> , <i>c</i> (Å)	41.6, 62.3, 86.2	41.5, 62.2, 86.1	41.7, 62.4, 86.7	41.5, 62.7, 86.1	41.5, 62.6, 86.1	41.5, 61.7, 86.7
$\alpha = \beta = \gamma$ (deg)	90	90	90	90	90	90
resolution range <sup>a</sup> (Å)	22.1–1.56 (1.62–1.56)	29.3–1.17 (1.21–1.17)	50.6–1.39 (1.42–1.39)	29.5–1.26 (1.31–1.26)	29.4–1.29 (1.33–1.29)	50–1.45 (1.48–1.45)
<i>R</i> <sub>merge</sub> (%)	2.2 (5.1)	1.4 (9.6)	7.0 (40.4)	1.8 (14.1)	1.9 (15.1)	6.1 (30.0)
<i>I</i> / $\sigma$ <i>I</i>	39.4 (12.2)	17.9 (4.3)	27.5 (4.7)	19.1 (4.9)	17.6 (4.4)	22.2 (5.0)
completeness (%)	100 (100)	99.9 (100)	99.9 (100)	99.7 (98.8)	96.8 (93.2)	98.9 (79.9)
Wilson B-factor (Å <sup>2</sup> )	9.90	9.18	8.39	9.25	9.16	11.64
Refinement						
molecules per asymmetric unit	1	1	1	1	1	1
no. of unique reflections	32 576	76 012	46 446	61 202	56 078	41 240
<i>R</i> <sub>work</sub> / <i>R</i> <sub>free</sub> (%)	14.2/16.2	12.6/14.3	15.3/18.1	16.2/18.2	16.1/18.4	16.1/18.0
no. of protein atoms	1962	1963	1957	1962	1961	1950
average B-factor (Å <sup>2</sup> )						
protein	10.12	12.20	10.08	11.33	10.85	12.63
solvent	24.55	30.30	22.52	23.47	22.88	22.53
ligand				17.10	13.90	16.2
RMS deviations						
bond length (Å)	0.006	0.005	0.006	0.005	0.006	0.005
bond angles (deg)	1.1	1.1	1.1	1.1	1.1	1.1
PDB codes	4PM6	4PM8	4PMA	4PMS	4PM7	4PM9

<sup>a</sup>Numbers in the parentheses indicate values for highest resolution shell.

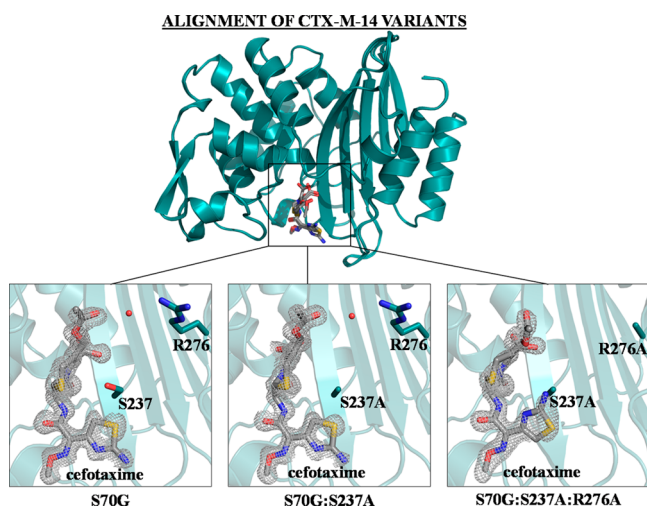


**Figure 3.** Electron density of cefotaxime in complex with the CTX-M-14 mutant enzymes. An alignment of CTX-M-14 mutants S70G, S70G:S237A, and S70G:S237A:R276A is shown on top, with the enzyme shown as teal ribbon and the substrate depicted as gray sticks. Below, the  $F_o - F_c$  difference map is shown in gray at  $3\sigma$ . CTX-M-14 positions 237 and 276 are shown as teal sticks, with the enzyme shown in ribbon and cefotaxime shown in gray. The water molecule that forms hydrogen bonds with both Arg276 and cefotaxime in the S70G and S70G:S237A structures is displayed as a red sphere. Nitrogen atoms are shown in blue, oxygen atoms are shown in red, and sulfur atoms are shown in yellow. Images generated in PyMOL.<sup>29</sup>

S70G:S237A:R276A mutants, respectively. The apoenzyme and cefotaxime-complexed structures show an RMSD of 0.12 Å for the  $C\alpha$  atoms of the active site for the single mutant, 0.10 Å for the double mutant, and 0.12 Å for the triple mutant, suggesting that the substrate did not induce substantial structural modifications to the enzyme. All of the CTX-M-14 structures obtained in this study crystallized in the same space group. A fluorescence scan was performed on CTX-M-14 and the S237A and S237A:R276A mutants in order to confirm that the proteins used for kinetic analysis also exhibit no large structural changes in solution that would affect intrinsic fluorescence (Supporting Information Figure S2).

Comparing the cefotaxime-bound CTX-M-14 mutant structures with a previously published structure of the CTX-M-9 S70G mutant complexed with cefotaxime (PDB ID: 3HLW) showed an RMSD of 0.21 Å for the  $C\alpha$  atoms in the active site for the single mutant, 0.21 Å for the double mutant, and 0.20 Å for the triple mutant, indicating that there are no major displacements of active site residues.<sup>11</sup> Lastly, in an alignment of all the residues, no residue exhibited greater than a 1 Å deviation when the cefotaxime-bound double and triple mutants were compared to the cefotaxime-bound S70G mutant.

**Interactions between the CTX-M-14 Mutant Enzymes and Cefotaxime.** The structure of the CTX-M-14 S70G enzyme in complex with cefotaxime maintains all of the same electrostatic and hydrophobic interactions between cefotaxime in the active site as those in the previously published structure of CTX-M-9 in complex with cefotaxime.<sup>11</sup> The previous structure of the CTX-M-9 enzyme in complex with cefotaxime, however, contains an additional cefotaxime molecule at the entrance to the active site that was proposed to indicate an entry site for the drug to the active site.<sup>11</sup> The additional cefotaxime molecule was not observed in our CTX-M-14

S70G–cefotaxime structure, which could be the result of crystallization in a different space group.

Comparing the structures of the cefotaxime complex of CTX-M-14 S70G (wild-type), S70G:S237A, and S70G:S237A:R276A shows four major structural differences resulting from the mutations. First, upon removal of the S237 hydroxyl group (S70G:S237A), the C4 carboxylate group of cefotaxime assumes an alternative position, moving closer to Lys234 than in the wild-type enzyme. Second, the aminothiazole ring of cefotaxime is flipped 180° in the S70G:S237A:R276A–cefotaxime structure, moving away from the binding site in the wild-type structure. Third, the hydrogen bond between Asn170(O) and Asp240(N), that is characteristic of the smaller TEM-1/SHV active site, is present in the wild-type and mutant apo enzymes. This hydrogen bond is broken when cefotaxime binds to the S70G and S70G:S237A enzymes; however, it is retained in the S70G:S237A:R276A–cefotaxime structure. Finally, the overall hydrogen-bonding network between cefotaxime and the active site in the S70G:S237A:R276A structure is diminished (Figure 4).

When Ser237 is mutated to the TEM/SHV-type residue, alanine, it eliminates the hydrogen bond observed in the wild-type (S70G) cefotaxime complex between the C4 carboxylate of cefotaxime with Ser237O' and Ser130O' (Figure 5A). As a result, the C4 carboxyl group shifts into the position occupied by a water molecule in the S70G–cefotaxime structure (Figure 5A). There, it participates in the same hydrogen bonds with Lys234(N2) and Lys73(N2) as the water molecule does in the S70G–cefotaxime structure. The vast majority of the hydrophobic interactions with cefotaxime are maintained between the S70G and S70G:S237A structures (Figure 4A,B). The position of the C4 carboxyl group near where the Ser70 oxygen would normally reside is, in part, due to the S70G substitution creating space for the carboxyl in this region. Nevertheless, the result indicates the loss of interaction with Ser237O' leads to repositioning of the C4 carboxyl group and a lower catalytic efficiency.

A previous comparison of the structure of the CTX-M-9 S70G apoenzyme with the cefotaxime-bound structure found that the hydrogen bond between Asn170(O) and Asp240(N) is ruptured to accommodate cefotaxime in the binding pocket.<sup>11</sup> It was hypothesized that breaking the Asn170–Asp240 hydrogen bond widens the active site to accommodate and position cefotaxime more optimally for catalysis. This hydrogen bond is also absent in the CTX-M-14 S70G–cefotaxime and S70G:S237A–cefotaxime structures reported here; however, when both Ser237 and Arg276 side chains are converted to alanine in the double mutant, the hydrogen bond between Asn170 and Asp240 is retained, even in the presence of cefotaxime. This narrows the active site in this region, making it more difficult for cefotaxime to achieve optimal positioning and decreasing  $k_{cat}/K_m$  for catalysis of cefotaxime (Figure 5B).

The removal of the side chains of Ser237 and Arg276 also allow the aminothiazole ring to flip 180° into a position that makes fewer contacts with the enzyme. The hydrogen bond between the Asp240 oxygen(Oε1) and the amino group on the aminothiazole is also lost (Figure 5B). The presence of the Ser237 hydroxyl group would be sufficient to sterically interfere with the aminothiazole ring in this flipped conformation; however, removing this steric clash is not sufficient to cause the ring to flip. The side chain of Arg276 must also be converted to alanine before the flip occurs. It is clear from this structural feature that Ser237 and Arg276 work cooperatively to stabilize



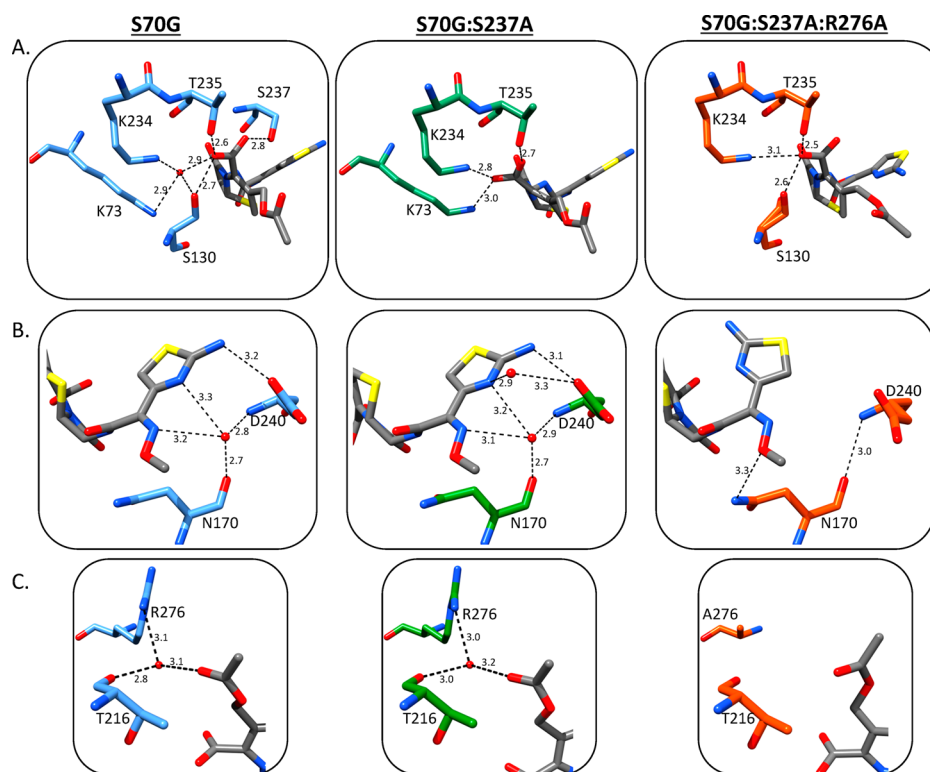


**Figure 5.** Hydrogen-bonding network between cefotaxime and the CTX-M-14 mutants. The enzyme in the S70G–cefotaxime structure is shown as blue sticks, S70G:S237A–cefotaxime structure is shown as green sticks, and S70G:S237A:R276A–cefotaxime structure is shown as orange sticks. Cefotaxime is shown as gray sticks throughout. Only residues that form hydrogen bonds with the C4 carboxylate or aminothiazole ring on cefotaxime are shown. Water molecules that form hydrogen bonds with both the substrate and enzyme are shown in red. All hydrogen bonds are depicted as black dotted lines and are labeled with their distance (Å). (A) C4 carboxylate group is shown with hydrogen bonds to CTX-M-14 residues indicated. (B) The hydrogen-bonding network between the cefotaxime aminothiazole ring and the mutant CTX-M-14 enzymes. (C) The hydrogen-bonding network between cefotaxime methyl acetate group and the mutant CTX-M-14 enzymes. Images generated in Chimera.<sup>30</sup>

the bound cefotaxime with the aminothiazole ring in a conformation that is more buried in the active site and forms more contacts with CTX-M-14 residues.

Overall, the hydrogen-bonding network between cefotaxime and the CTX-M-14 enzyme is compromised in the S70G:S237A:R276A–cefotaxime structure as compared to the others (Figure 4C). In the pseudo-wild-type S70G–cefotaxime complex, cefotaxime is anchored into the active site by 12 hydrogen bonds involving 7 residues and 3 water molecules and hydrophobic interactions with 5 residues. In the S70G:S237A:R276A–cefotaxime structure, however, cefotaxime is anchored into the active site by only 9 hydrogen bonds involving 8 enzyme residues and no water molecules as well as hydrophobic interactions with 6 residues (Figure 4C). The absence of interactions between cefotaxime and the enzyme mediated by hydrogen bonding to water molecules in the S70G:S237A:R276A structure is related to the fact that these interactions in the other structures involve bonds with the aminothiazole ring of cefotaxime, which are lost with the 180° rotation of the ring in the triple mutant (Figures 4C and 5B). It is also interesting to note that these changes in water structure and hydrogen bonding are distant from the Ser237 and Arg276 substitutions. Thus, the changes in interactions with substrate at the site of substitution propagate to change interactions far from the site of mutation.

The hydrogen bond between the C3 methyl acetate group and water is lost in the S70G:S237A:R276A structure, which could lead to increased flexibility of this group, resulting in the slightly different placement in the active site (Figure 5C). A

comparison of the average B-factors of the C3 methyl acetate group in the three structures shows averages of 21.2, 13.9, and 27.9 Å<sup>2</sup> for the single, double, and triple mutants in complex with cefotaxime, respectively. This supports the notion that loss of the hydrogen bond between the C3 methyl acetate group and water slightly increases flexibility of this region. The overall B-factors for cefotaxime in the S70G, S70G:S237A, and S70G:S237A:R276A structure are 17.1, 13.9, and 16.2 Å<sup>2</sup>, respectively.

In summary, the retention of the Asn170–Asp240 hydrogen bond, flipping of the aminothiazole ring of cefotaxime, increased flexibility of the C3 methyl acetate group, and the absence of waters that bridge interactions between the substrate and the enzyme results in reduced hydrogen bonding and hydrophobic interactions, a narrower binding pocket, and a 14–29-fold reduction in  $k_{\text{cat}}/K_{\text{m}}$  for cefotaxime hydrolysis. Cumulatively, these changes in the positioning and bonding network of cefotaxime in the active site support the cooperative nature of positions Ser237 and Arg276 and highlight their contributions to enhancing cefotaxime hydrolysis in the CTX-M enzymes.

## DISCUSSION

The CTX-M family of  $\beta$ -lactamases is a widespread source of resistance to extended-spectrum cephalosporin antibiotics among Gram-negative bacteria. A distinguishing feature of the CTX-M enzymes compared to other class A  $\beta$ -lactamases, such as the commonly occurring TEM-1 and SHV-1 enzymes, is their ability to efficiently hydrolyze cefotaxime. The CTX-M

enzymes are also distinguished by the conservation of the active site residues Ser237 and Arg276 in that this combination does not occur in other class A  $\beta$ -lactamases.<sup>14</sup> In this study, we have used kinetic and structural methods to show that Ser237 and Arg276 act cooperatively to promote cefotaxime hydrolysis through structural alterations of the active site that better accommodate the larger cefotaxime molecule. As a result, these residues contribute to the unique substrate specificity of the CTX-M family of enzymes.

The X-ray crystal structures of the CTX-M-14 S70G, S70G:S237A, and S70G:S237A:R276A mutants with and without cefotaxime bound revealed that the mutations result in flipping of the aminothiazole ring 180°, decreased hydrogen bonding with the enzyme, and, importantly, a hydrogen bond between Asn170 and Asp240 that is retained when cefotaxime is bound. Previous work by Delmas et al. indicated that binding of cefotaxime in CTX-M-9  $\beta$ -lactamase results in a conformational change in the active site involving rupture of a hydrogen bond between main chain groups of Asn170 and Asp240 that connects the omega loop to the  $\beta$ 3 strand.<sup>11</sup> The net result of this change is to expand the active site to allow adequate positioning of the cefotaxime substrate for catalysis, which was hypothesized to contribute to the cefotaximase activity of the CTX-M enzymes.<sup>11</sup> The results of this study support this model since the preservation of this hydrogen bond in the S70G:S237A:R276A–cefotaxime complex is associated with a significant loss of activity as a cefotaximase (14-fold).

As noted above, Ser237 and Arg276 act cooperatively to increase  $k_{\text{cat}}/K_m$  for cefotaxime hydrolysis despite the fact that they are more than 8 Å apart and not within direct contact distance. Wells et al. analyzed the additivity of approximately 25 double mutations that were beyond van der Waals contact distance in the wild-type structures of several enzymes.<sup>31</sup> In these cases, the effects of the double mutation on binding and/or catalysis were largely additive, suggesting that the effects of mutating residues that do not directly interact with each other, as is the case for Ser237 and Arg276, are largely additive. Nonadditive effects were generally attributed to direct or indirect interactions of the two residues mediated through the protein or changes in mechanism.<sup>31</sup> A comparison of the X-ray structures of S70G–cefotaxime and S70G:S237A–cefotaxime versus S70G:S237A:R276A–cefotaxime shows changes in substrate orientation and hydrogen bonding, as described above (Figure 5). On the basis of these results, it appears that the cooperative effect between S237A and R276A is mediated indirectly through the substrate, i.e., although the residues are not in direct contact, they are bridged through contact with cefotaxime in the enzyme–substrate complex. Thus, Ser237, Arg276, and cefotaxime together form a connected, cooperative unit.

The S237A:R276N double mutation of CTX-M-14 suggests the cooperative interactions of Ser237 and Arg276 with cefotaxime contributes approximately 30-fold to enhancing hydrolysis compared to the TEM-1/SHV1-like active site. Given that the overall sequence identity of the two enzymes is only ~35%, the rest of the sequence changes must contribute an additional rate enhancement of 30-fold to account for the approximately 1000-fold ratio in  $k_{\text{cat}}/K_m$  for hydrolysis of cefotaxime catalyzed by CTX-M-14 compared to its hydrolysis by TEM-1. Therefore, there may be additional positions that contribute to the unique cefotaximase substrate specificity of the CTX-M enzymes.

In conclusion, CTX-M-14 residues Ser237 and Arg276 work together in the hydrolysis of  $\beta$ -lactam substrates to help shape the substrate specificity of the enzyme to that of an effective cefotaximase. The crystal structures of the CTX-M-14 S70G, S70G:S237A, and S70G:S237A:R276A mutants alone and in complex with cefotaxime revealed the importance of residues Ser237 and Arg276 in establishing the interactions with cefotaxime and cooperatively shaping the active site in the region of Asn170 and Asp240. Finally, the results suggest the cooperative interaction between Ser237 and Arg276 is mediated via an indirect interaction bridging through the cefotaxime substrate. Cooperative interactions among residues that contact the substrate or transition state may serve as useful points for engineering protein–small molecule interactions for binding or for catalysis.

## ■ ASSOCIATED CONTENT

### Supporting Information

Table S1: MICs of CTX-M-14  $\beta$ -lactamase and mutant enzymes. Figure S1: Catalytic efficiency of CTX-M-14  $\beta$ -lactamase and mutant enzymes. Figure S2: Fluorescence scan of CTX-M-14  $\beta$ -lactamase and mutant enzymes. This material is available free of charge via the Internet at <http://pubs.acs.org>.

### Accession Codes

The coordinates of the structures reported in this article have been deposited in the Protein Data Bank ([www.rcsb.org](http://www.rcsb.org)) (PDB ID codes 4PMS, 4PM6, 4PM7, 4PM8, 4PM9, and 4PMA).

## ■ AUTHOR INFORMATION

### Corresponding Author

\*Phone: 713-798-5609; Fax: 713-798-7375; E-mail: [timothy@bcm.tmc.edu](mailto:timothy@bcm.tmc.edu).

### Author Contributions

<sup>†</sup>C.J.A. and A.M.C. contributed equally to this work.

### Funding

This work was supported by a training fellowship from the Houston Area Molecular Biophysics Training Program (NIGMS grant no. T32 GM008280) of the Gulf Coast Consortia to C.J.A., a training fellowship from the Keck Center of Biomedical Discovery Training Program of the Gulf Coast Consortia (NIH grant no. 1 R90 DA023418-03) to A.M.C., and a training fellowship from the Keck Center of Pharmacoinformatics Training Program of the Gulf Coast Consortia (NIH grant no. T90 DK070109-05) to N.G.B. This work was supported by NIH grant no. AI32956 to T.P. B.V.V.P. acknowledges support from Robert Welch Foundation (Q1279). This work was supported by The Berkeley Center for Structural Biology, supported in part by the National Institutes of Health, National Institute of General Medical Sciences, and the Howard Hughes Medical Institute. The Advanced Light Source is supported by the Director, Office of Science, Office of Basic Energy Sciences, of the U.S. Department of Energy under contract no. DE-AC02-05CH11231.

### Notes

The authors declare no competing financial interest.

## ■ ABBREVIATIONS

ESBL, extended spectrum  $\beta$ -lactamases; BLIP-II,  $\beta$ -lactamase inhibitory protein II; MIC, minimum inhibitory concentration

## REFERENCES

- (1) Fisher, J. F., Meroueh, S. O., and Mobashery, S. (2005) Bacterial resistance to beta-lactam antibiotics: compelling opportunism, compelling opportunity. *Chem. Rev.* 105, 395–424.
- (2) Ambler, R. P., Coulson, F. W., Frere, J.-M., Ghuysen, J.-M., Joris, B., Forsman, M., Levesque, R. C., Tiraby, G., and Waley, S. G. (1991) A standard numbering scheme for the class A  $\beta$ -lactamases. *Biochem. J.* 276, 269–272.
- (3) Bush, K., and Fisher, J. F. (2011) Epidemiological expansion, structural studies, and clinical challenges of new  $\beta$ -lactamases from Gram-negative bacteria. *Annu. Rev. Microbiol.* 65, 455–478.
- (4) Bonnet, R. (2004) Growing group of extended-spectrum beta-lactamases: the CTX-M enzymes. *Antimicrob. Agents Chemother.* 48, 1–14.
- (5) Chen, Y., Delmas, J., Sirot, J., Shoichet, B. K., and Bonnet, R. (2005) Atomic resolution structures of CTX-M beta-lactamases: extended spectrum activities from increased mobility and decreased stability. *J. Mol. Biol.* 348, 349–362.
- (6) Canton, R., Gonzalez-Alba, J. M., and Galan, J. C. (2012) CTX-M enzymes: origin and diffusion. *Front. Microbiol.* 3, 1–19.
- (7) Orenca, M. C., Yoon, J. S., Ness, J. E., Stemmer, W. P., and Stevens, R. C. (2001) Predicting the emergence of antibiotic resistance by directed evolution and structural analysis. *Nat. Struct. Biol.* 8, 238–242.
- (8) Wang, X., Minasov, G., and Shoichet, B. K. (2002) Evolution of an antibiotic resistance enzyme constrained by stability and activity trade-offs. *J. Mol. Biol.* 320, 85–95.
- (9) Ibuka, A., Taguchi, A., Ishiguro, M., Fushinobu, S., Ishii, Y., Kamitori, S., Okuyama, K., Yamaguchi, K., Konno, M., and Matsuzawa, H. (1999) Crystal structure of the E166A mutant of extended-spectrum  $\beta$ -lactamase Toho-1 at 1.8 Å resolution. *J. Mol. Biol.* 285, 2079–2087.
- (10) Ibuka, A. S., Ishii, Y., Galleni, M., Ishiguro, M., Yamaguichi, K., Frere, J. M., Matsuzawa, H., and Sakai, H. (2003) Crystal structure of extended-spectrum beta-lactamase Toho-1: insights into the molecular mechanism for catalytic reaction and substrate specificity expansion. *Biochemistry* 42, 10634–10643.
- (11) Delmas, J., Leyssene, D., Dubois, D., Birck, C., Vazeille, E., Robin, F., and Bonnet, R. (2010) Structural insights into substrate recognition and product expulsion in CTX-M enzymes. *J. Mol. Biol.* 400, 108–120.
- (12) Delmas, J., Chen, Y., Prati, F., Robin, F., Shoichet, B. K., and Bonnet, R. (2008) Structure and dynamics of CTX-M enzymes reveal insights into substrate accommodation by extended-spectrum beta-lactamases. *J. Mol. Biol.* 375, 192–201.
- (13) Perez-Llarena, F. J., Carelle, M., Mallo, S., Beceiro, A., Perez, A., Villanueva, R., Romero, A., Bonnet, R., and Bou, G. (2008) Structure-function studies of arginine at position 276 in CTX-M  $\beta$ -lactamases. *J. Antimicrob. Chemother.* 61, 792–797.
- (14) Marciano, D. C., Brown, N. G., and Palzkill, T. (2009) Analysis of the plasticity of location of positive charge within the active site of the TEM-1  $\beta$ -lactamase. *Protein Sci.* 18, 2080–2089.
- (15) Strynadka, N. C. J., Adachi, H., Jensen, S. E., Johns, K., Sielecki, A., Betzel, C., Sutoh, K., and James, M. N. G. (1992) Molecular structure of the acyl-enzyme intermediate in  $\beta$ -lactam hydrolysis at 1.7 Å resolution. *Nature* 359, 700–705.
- (16) Wang, X., Minasov, G., and Shoichet, B. K. (2002) The structural bases of antibiotic resistance in clinically derived mutant beta-lactamases TEM-30, TEM-32 and TEM-34. *J. Biol. Chem.* 277, 32149–32156.
- (17) Zafaralla, G., Manavathu, E. K., Lerner, S. A., and Mobashery, S. (1992) Elucidation of the role of arginine-244 in the turnover processes of class A beta-lactamases. *Biochemistry* 31, 3847–3852.
- (18) Gazouli, M., Legakis, N. J., and Tzouveleki, L. S. (1998) Effect of substitution of Asn for Arg-276 in the cefotaxime-hydrolyzing class A  $\beta$ -lactamase CTX-M-4. *FEMS Microbiol. Lett.* 169, 289–293.
- (19) Gazouli, M., Tzelepi, E., Sidorenko, S. V., and Tzouveleki, L. S. (1998) Sequence of the gene encoding a plasmid-mediated cefotaxime-hydrolyzing class A  $\beta$ -lactamase (CTX-M-4): involvement of serine 237 in cephalosporin hydrolysis. *Antimicrob. Agents Chemother.* 42, 1259–1262.
- (20) Brown, N. G., Chow, D., Ruprecht, K. E., and Palzkill, T. (2013) Identification of the  $\beta$ -lactamase inhibitor protein-II (BLIP-II) interface residues essential for binding affinity and specificity for class A  $\beta$ -lactamases. *J. Biol. Chem.* 288, 17156–17166.
- (21) Copeland, R. A. (2000) *Enzymes: A Practical Introduction to Structure, Mechanism, and Data Analysis*, 2nd ed., Wiley-VCH, New York.
- (22) Batty, T. G., Kontogiannis, L., Johnson, O., Powell, H. R., and Leslie, A. G. (2011) iMOSFLM: a new graphical interface for diffraction-image processing with MOSFLM. *Acta Crystallogr., Sect. D: Biol. Crystallogr.* 67, 271–281.
- (23) Collaborative Computational Project (1994) The CCP4 suite: programs for protein crystallography. *Acta Crystallogr., Sect. D: Biol. Crystallogr.* 50, 760–763.
- (24) Vagin, A., and Teplyakov, A. (1997) MOLREP: an automated program for molecular replacement. *J. Appl. Crystallogr.* 30, 1022–1025.
- (25) McCoy, A. J., Grosse-Kunstleve, R. W., Adams, P. D., Winn, M. D., Storoni, L. C., and Read, R. J. (2007) Phaser crystallographic software. *J. Appl. Crystallogr.* 40, 658–674.
- (26) Otwinowski, Z., and Minor, W. (1997) Processing of X-ray diffraction data collected in oscillation mode, in *Methods in Enzymology: Macromolecular Crystallography, Part A* (Carter, C. W., and Sweet, R. M., Eds.) pp 307–326, Academic Press, New York.
- (27) Emsley, P., and Cowtan, K. (2004) Coot: model-building tools for molecular graphics. *Acta Crystallogr., Sect. D: Biol. Crystallogr.* 60, 2126–2132.
- (28) Laskowski, R. A., and Swindells, M. B. (2011) LigPlot+: multiple ligand-protein interaction diagrams for drug discovery. *J. Chem. Inf. Model.* 51, 2778–2786.
- (29) *The PyMOL Molecular Graphics System*, version 1.3, Schrödinger, LLC.
- (30) Pettersen, E. F., Goddard, T. D., Huang, C. C., Couch, G. S., Greenblatt, D. M., Meng, E. C., and Ferrin, T. E. (2004) UCSF Chimera—a visualization system for exploratory research and analysis. *J. Comput. Chem.* 25, 1605–1612.
- (31) Wells, J. (1990) Additivity of mutational effects in proteins. *Biochemistry* 29, 8509–8517.